Provided for non-commercial research and education use.
Not for reproduction, distribution or commercial use.

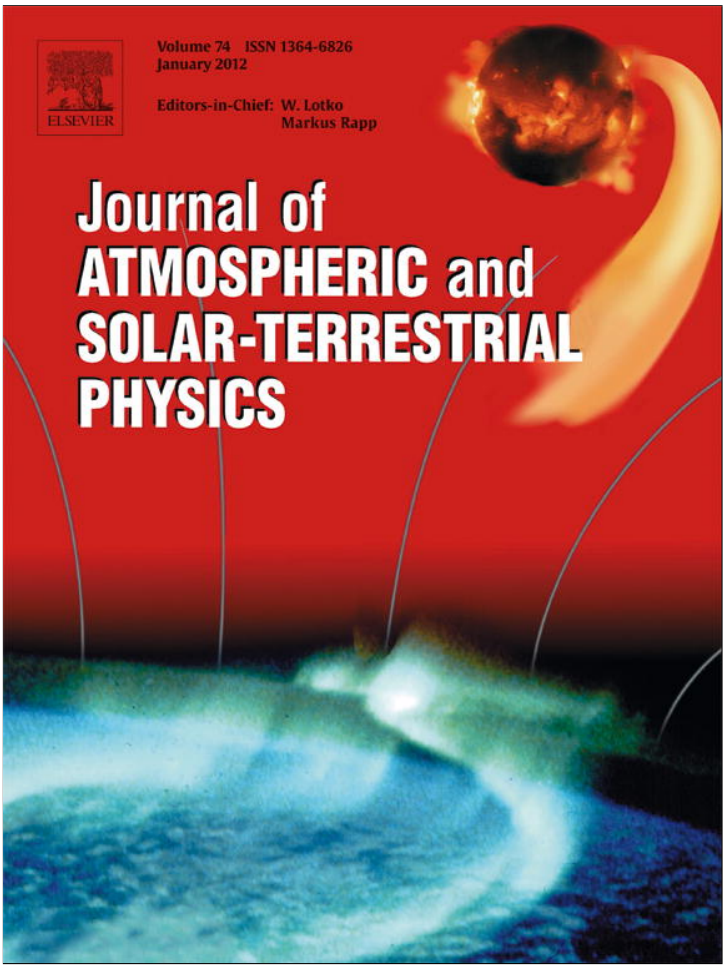

This article appeared in a journal published by Elsevier. The attached copy is furnished to the author for internal non-commercial research and education use, including for instruction at the authors institution and sharing with colleagues.

Other uses, including reproduction and distribution, or selling or licensing copies, or posting to personal, institutional or third party websites are prohibited.

In most cases authors are permitted to post their version of the article (e.g. in Word or Tex form) to their personal website or institutional repository. Authors requiring further information regarding Elsevier's archiving and manuscript policies are encouraged to visit:

http://www.elsevier.com/authorsrights

Author's personal copy

Journal of Atmospheric and Solar-Terrestrial Physics 102 (2013) 222–227

Contents lists available at SciVerse ScienceDirect

Journal of Atmospheric and Solar-Terrestrial Physics

journal homepage: www.elsevier.com/locate/jastp

Widths of dayside auroral arcs observed at the Chinese Yellow River Station

Qi Qiu [a,b,*], Hui-Gen Yang [a], Quan-Ming Lu [b], Qing-He Zhang [a], De-Sheng Han [a], Ze-Jun Hu [a]

[a] SOA Key Laboratory for Polar Science, Polar Research Institute of China, Shanghai 200136, China
[b] CAS Key Laboratory of Basic Plasma Physics, Department of Geophysics and Planetary Science, University of Science and Technology of China, Hefei 230026, China

ARTICLE INFO

Article history:
Received 5 September 2012
Received in revised form
3 June 2013
Accepted 5 June 2013
Available online 14 June 2013

Keywords:
Auroral arc
Observed width
Corrected width

ABSTRACT

Due to the altitudinal extent of an auroral arc, its observed width is different at different zenith angles even when its real width is the same. For that reason, former measurements of arc widths were obtained only for arcs located close to the geomagnetic zenith direction. A method to correct arc width is proposed in the paper, which considers the altitudinal extent of auroral arc. Then, we apply this method to the auroral arcs observed at the Chinese Yellow River Station, and analyze the widths of 17,571 dayside auroral arcs. The distributions of the widths are almost the same at different zenith angles with an average width of 18.5 km. Arc widths are narrower as MLT is close to midday.

© 2013 Published by Elsevier Ltd.

1. Introduction

The auroral oval appears as a continuous ring of emissions encircling the geomagnetic pole (Yang et al., 2000), in which complex forms of discrete aurora (Akasofu, 1976; Rostoker et al., 1987; Murphree et al., 1987) are frequently found to be embedded in a broader, less structured diffuse aurora (Lui and Anger, 1973). Auroral arc is one of typical forms of discrete aurora in the prenoon and postnoon sectors (Sandholt et al., 2002). It is the typical track of the interaction between solar wind and the earth magnetosphere, which is also an indicator of the activity of the space weather. Spatial scale of the auroral arc is one of the most important factors in understanding auroral morphology (Borovsky, 1993), which is associated with the scale of the various dynamic processes in magnetospheric boundary layer.

Kim and Volkman (1963) found that the characteristic width of the stable auroral arcs is of the order of 10 km after they analyzed 40 stable arcs, which were observed with wide-angle lenses. Later, Maggs and Davis (1968), and Borovsky et al. (1991) identified a population of arcs with a characteristic width of 100 m with narrow-field TV cameras. However, Stenbaek-Nielsen et al. (1999) noticed that a significant fraction of them were in fact taken inside the region of the diffuse aurora. Recently, Knudsen et al. (2001) analyzed widths of 3126 stable auroral arcs observed by an all-sky camera located in Gillam, Manitoba, and chose these mesoscale arcs which were located within $\pm 5^\circ$ of magnetic zenith, and found that the average width is about 18 km with a standard deviation of about 9 km.

However, all previous studies only considered the arcs near the magnetic zenith, where the effect of the altitudinal extent of arcs is negligible. This would reduce largely the available number of arc samples and would be hard to study the evolution features of the arc. In this paper, we propose a method to correct the effect of the altitudinal extent of arcs. Therefore, the method can be used to calculate the width of an arc in regions with much larger zenith angles. At last, we analyze 17,571 dayside auroral arcs obtained at the Yellow River Station in 2003 with this method and discuss how arc widths varied with MLT.

2. Data and methodology

2.1. Observation data

The data used in this study were collected during 0600–1800 MLT from November 18, 2003 to January 31, 2004 with an all-sky camera at the Chinese Yellow River Station (YRS), at Ny-Ålesund, Svalbard. YRS is located at 78.92°N in the geographic coordinate with 76.24° geomagnetic latitude (MLAT), and MLT≈UT+3 h (Hu et al., 2009). The camera uses a 512×512 square pixel array, and the center of the field of view is geographic zenith. It has single-pixel spatial resolutions from 1.1 km to 2.1 km as the zenith

* Corresponding author. Tel.: +86 21 58715494; fax: +86 21 58715031.
E-mail addresses: qiuqi@pric.gov.cn (Q. Qiu), huigen_yang@pric.gov.cn (H.-G. Yang), qmlu@ustc.edu.cn (Q.-M. Lu), zhangqinghe@pric.gov.cn (Q.-H. Zhang), Handesheng@pric.gov.cn (D.-S. Han), Huzejun@pric.gov.cn (Z.-J. Hu).

1364-6826/$ - see front matter © 2013 Published by Elsevier Ltd.
http://dx.doi.org/10.1016/j.jastp.2013.06.002

Author's personal copy

angle is from 0° to 45° with an average spatial resolution of 1.35 km (at 150 km). All-sky images (ASIs) are taken with a 7 s exposure time every 10 s, using a 5577 Å filter having a bandwidth of 20 Å.

2.2. Data analysis method

The discrete and stable auroral arcs were identified in aurora image sequences by eye. Although the surveyed interval was limited to 0600–1800 MLT, the arcs we selected did not occur in the midday sector because of the midday gap, and most of them occurred in the postnoon sector. The normal direction to the arc was determined, and then an intensity variation curve was drawn by extracting along this direction to measure arc width. A first estimation of the cross-arc direction was made interactively, and then refined automatically by rotating the line passing through the zenith to find the nearest point in the arc away from the zenith. This point was the minimum zenith angle of the peak. When we draw the intensity variation curve, the intensity was normalized with the maximum value of ASI. In Fig. 1b, some small fluctuations marked with red circles are not auroral arcs. In order to avoid the effect of these small fluctuations, these small peaks would also be ignored when the discrepancy between the peak and the valley was less than 0.1. The peak satisfying the 0.1 peak-to-valley criteria was corresponding to an arc. Thus, the observed arc width was defined as the distance between two pixels with nearly equal intensities at half maximum points.

Fig. 1a is a multiple arcs image taken at YRS, December 31, 2003, at 1330UT. From Fig. 1a, we can identify four auroral arcs, the red point in the center is the geographic zenith, and the red line is the normal direction to the fourth arc. The normal directions to the other arcs are nearly the same. An intensity variation curve is drawn in Fig. 1b by extracting along this line. In Fig. 1b, four peaks represent four arcs, and the zenith angle of peak is defined to be the zenith angle of the arc. The first arc is not considered, and the reason will be described below. The widths of the other arcs are the distance between arrows.

In all-sky image, every pixel has the same solid angle. Using the trigonometric relations, the distance d away from the zenith and the geocentric angle α varies with the corresponding zenith angle θ and is given as

$$\alpha = \theta - \sin^{-1}\left[\frac{R_E}{R_E + h}\sin\theta\right] \quad (1)$$

$$d = (R_E + h)\alpha \quad (2)$$

where R_E is the earth radius and h is the altitude of aurora emission. In this study, R_E is 6370 km and auroral altitude h is assumed to be 150 km. Using Eqs. (1) and (2), we can find that distance d varies approximately linearly with zenith angle θ when the absolute value of the zenith angle is smaller than 45°, but becomes a non-linear relationship when zenith angle is larger than 45°. So we do not consider these arcs in this paper if the absolute value of their zenith angle is larger than 45°. When zenith angle θ is 45°, geocentric angle α is 1.3°.

Because of the altitudinal extent of an arc, the observed arc width is not the real width of the arc, especially for the arc away from the zenith. The observed arc width w consists of two parts: the real arc width w_0 and an additional arc width Δw due to the

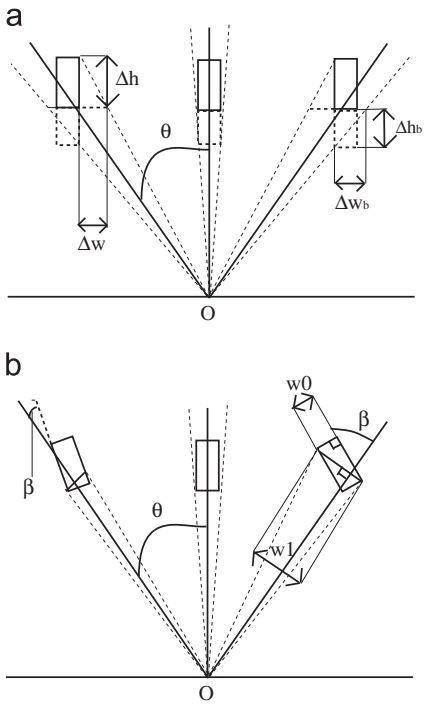

Fig. 2. Sketch map of the correction method to calculate arc widths. θ is the zenith angle of the arc, Δh is the altitudinal extent of the arc, and β is the angle between the field-parallel direction and the direction of the line of sight.

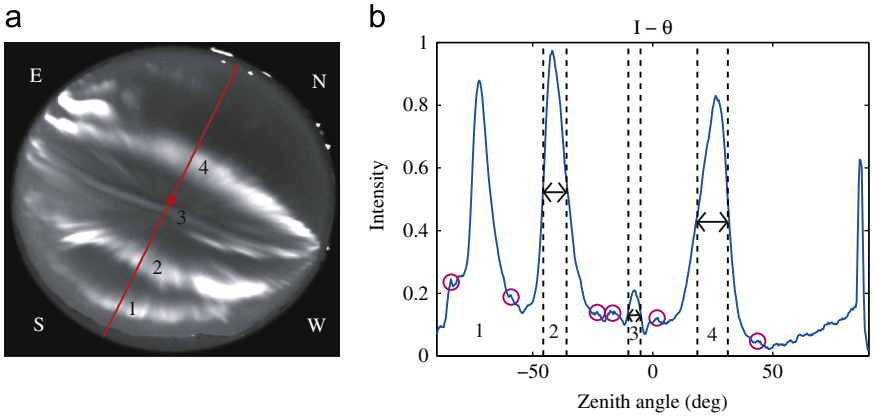

Fig. 1. (a) Multiple arcs image with an all-sky camera (5577 Å, ASI) taken at the Yellow River Station, December 26, 2003, at 1330UT. The red point in the center of image is geographic zenith and the red line is the normal direction to arcs. (b) The solid line is intensity variation curve along the normal direction to arcs. Any peak is corresponding to an arc. The width of the arc is the distance between arrows. (For interpretation of the references to color in this figure legend, the reader is referred to the web version of this article.)

Author's personal copy

altitudinal extent Δh. Fig. 2a shows that Δw is given by

$$\Delta w = \Delta h|\tan\ \theta| \tag{3}$$

Considering that auroral particles precipitate into the polar ionosphere along the magnetic field lines, zenith angle in Eq. (3) should be changed to geomagnetic zenith angle

$$\Delta w = \Delta h|\tan(\theta-\theta_{mz})| \tag{4}$$

where θ_{mz} is the angular distance from geomagnetic zenith to geographic zenith.

We define angle β as the angular distance between the magnetic field direction and the line-of-sight (LOS) direction. Fig. 2b shows that we will overestimate the width because of the effect of angle β. The relation can be given as

$$w = w_1 + \Delta w = w_0/\cos\ \beta + \Delta w \tag{5}$$

where we assume that angle β varies linearly with the zenith angle θ. This assumption is checked later in the article.

$$\beta = k(\theta-\theta_{mz}) \tag{6}$$

Because β is related to the magnetic field direction, k is different for the positive and negative geomagnetic zenith.

Taking Eqs. (4) and (6) into account, the relationship between observed width and real width (Eq. (5)) could be given as

$$w = w_0/\cos\left[k(\theta-\theta_{mz})\right] + \Delta h|\tan(\theta-\theta_{mz})| \tag{7}$$

$$w_0 = \left[w-\Delta h|\tan(\theta-\theta_{mz})|\right]\cos\left[k(\theta-\theta_{mz})\right] \tag{8}$$

where the coefficient k and the altitudinal extent of aurora emission Δh can be obtained from least square fitting to the data. Using Eqs. (7) and (8), we can calculate the real width of an arc.

3. The distribution of the arc widths

Fig. 3 is a scatter plot of full widths at half maximum (FWHM) for 17,571 arcs, organized according to the geographic zenith angle along the normal direction to arcs. The upper and lower blue lines are respectively the average FWHM and the minimum FWHM curves as a function of zenith angle. The average FWHM is the average of arc widths observed within $\pm 0.5^\circ$ of the zenith angle. The minimum FWHM is the average of three minimum widths of arcs observed within $\pm 0.5^\circ$. From Fig. 3, we find that the narrowest arc is at nearly -8.9° geographic zenith angle corresponding to the geomagnetic zenith. Average arc width increases as the zenith angle moves away from this point. This trend is the result of altitudinal extent of arcs. The real width w_0 is assumed as the observed value at geomagnetic zenith and Δh is assumed independent on the zenith angle. Using Eq. (7) to perform least square fit (LSF) on average and the minimum FWHM curve at the positive and negative geomagnetic zenith, we could obtain altitudinal extent Δh and k. In Eq. (7), Δh item has the same order of magnitude as w_0 item for the average FWHM, but Δh item is much larger than w_0 item for the minimum FWHM. Hence we used average and minimum FWHM to obtain Δh but only used average FWHM to obtain k. The detail step is: perform LSF on average and the minimum FWHM curve at the positive and negative geomagnetic zenith respectively, we could obtain four different values of the altitudinal extent Δh; then we chose the altitudinal extent Δh to be the average value of these four values and it is 30 km; and after that, we used Eq. (7) and $\Delta h = 30$ to fit on the average FWHM curve again, and we obtained k as 2.3 and 1.4 for the positive and negative geomagnetic zenith respectively. The upper and lower red lines are respectively the average width and the minimum width calculated by Eq. (7). Comparing the red and blue lines, the calculated values using Eq. (7) are roughly consistent with the FWHM with correlation coefficients of about 0.87 and 0.94 for the average and minimum width respectively. But, the correlation coefficients are 0.99 and 0.97 and average errors on FWHM are 1.89 km and 1.63 km, if we only consider these arcs with zenith angles between -38° and 42°.

Then, we would discuss the specific applicable scope and error of this method. For any zenith angle, data were taken from arcs within $\pm 0.5^\circ$ around this zenith angle. The widths of all arcs were corrected using Eq. (8). Fig. 4 shows average width of auroral arcs as a function of zenith angle (solid line). Average widths are nearly the same and their mean value is 17.7 km (plotted with horizontal dashed line) as the absolute value of zenith angle is less than 20°. The dotted lines indicate the pixel resolution away from this average value. Although the average width is a bit larger near zenith angle of $\pm 30^\circ$, the discrepancy away from this average width is almost less than the pixel resolution as zenith angle varies from -38° to 42° (between two vertical dashed-dotted lines). But the discrepancy is too large when zenith angle is less than -38° or

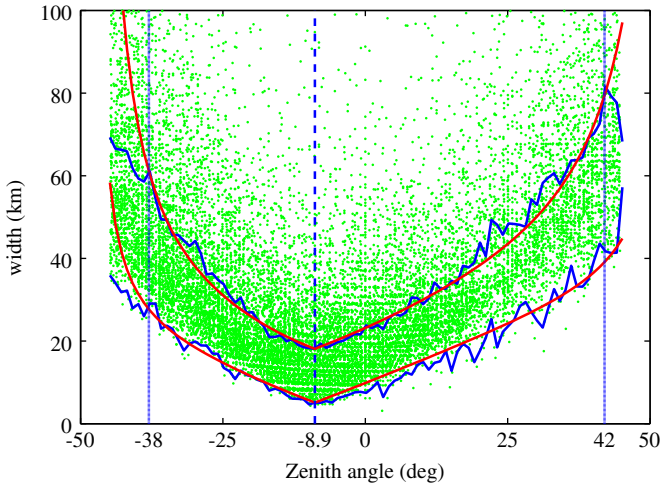

Fig. 3. The widths between intensity half maximum points for 17,571 auroral arcs, plotted as a function of zenith angle along the normal direction to arcs. The upper and lower blue lines are respectively the observed average width and minimum width variation curves. The upper and lower red lines are respectively the average width and minimum width variation curves calculated by Eq. (7). (For interpretation of the references to color in this figure legend, the reader is referred to the web version of this article.)

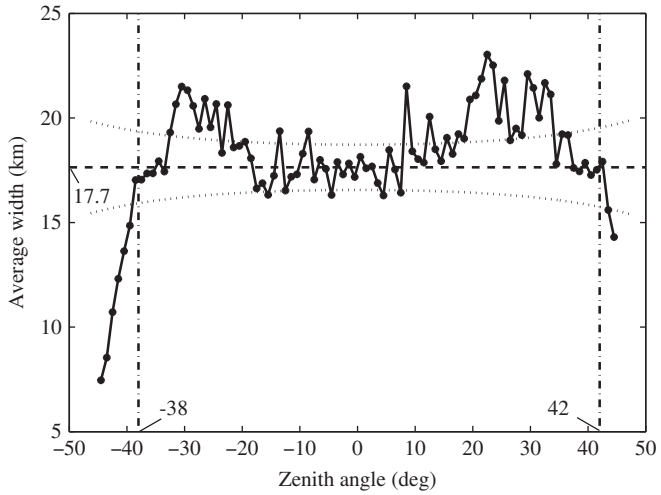

Fig. 4. Average width of auroral arcs as a function of zenith angle (solid line). The horizontal dashed line indicates the mean value of average widths between -20° zenith angle and 20° zenith angle. The dotted line shows the pixel resolution away from this mean value. The vertical dashed-dotted line is corresponding to -38° zenith angle and 42° zenith angle.

Author's personal copy

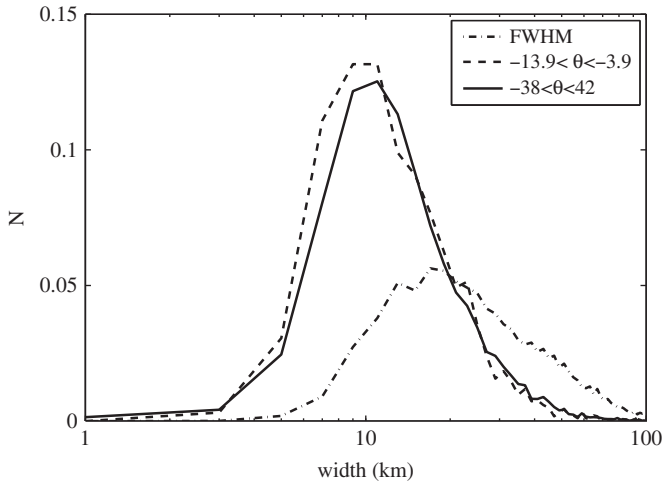

Fig. 5. Distributions of arc widths. The dashed-dotted line shows FWHM for all data, the solid line and dashed line show widths corrected by Eq. (8) for data points taken respectively within confidence interval, and those within $\pm 5^\circ$ of -8.9° zenith angle (geomagnetic zenith).

it is larger than 42°. So the confidence interval of this correction method is between −38° and 42°.

Fig. 5 shows distributions of arc widths. The dashed-dotted line shows FWHM for all the observations, the solid line and dashed line show widths corrected by Eq. (8) for data points taken respectively within confidence interval, and those within $\pm 5^\circ$ of -8.9° zenith angle (near geomagnetic zenith). From Fig. 5, we can find that the solid line is roughly consistent with the dashed line. Comparing the dashed dotted line with these two lines, the distribution is obviously different, the number of wider arcs is larger and the average width is 37 km. It means that the width is much bigger because the altitudinal extent of the arc is mixed with arc width. It is worth noting that the average width for the arcs taken within confidence interval and that of the arcs within $\pm 5^\circ$ of geomagnetic zenith is18.5 km and 17.7 km with standard deviations of 12.9 km and 12.6 km, which is consistent with the full observation widths of 18 ± 9 km within $\pm 5^\circ$ of geomagnetic zenith reported by Knudsen et al. (2001). This suggests that the widths calculated using Eq. (8) approximate well the real widths and can be applied to larger zenith angles.

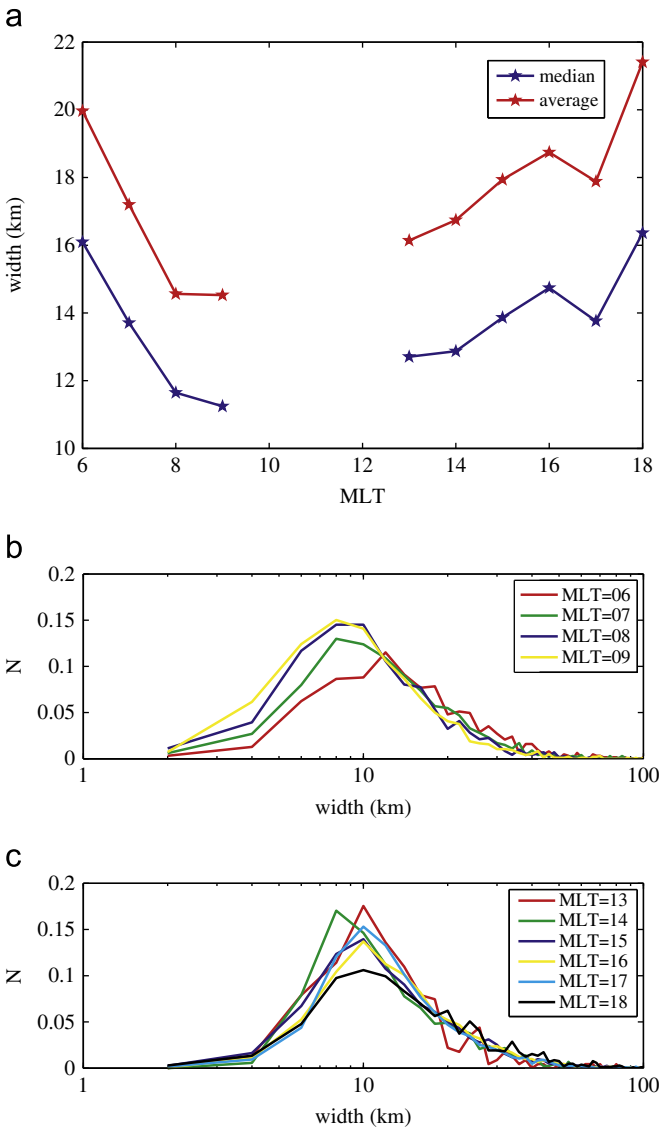

Fig. 6. (a) Average width and median width varied with MLT. (b) Distributions of arc widths in the prenoon sector. (c) Distributions of arc widths in the postnoon sector.

4. Arc widths variation in different MLT

In this section we would study the variation of corrected arc widths in different MLT. Average and median arc width variation curves with MLT are shown in Fig. 6a. No data were used at midday because of midday gap. Distributions of arc widths in the prenoon sector and in the postnoon sector were shown in Fig. 6b and c respectively. From Fig. 6a, we can see that average width and median width decreased with time progress in the prenoon and increased in the postnoon. Average width is smallest as MLT is close to midday. Auroral particles were precipitated from magnetospheric source region along magnetic field line. So arc width is mapped according to flux conservation

$$B_{ion}L_{ion}W_{ion} = B_{mag}L_{mag}W_{mag} \tag{9}$$

where B is the magnetic induction, L is the length of the structure, and W is the width of the structure, and where the subscripts "*ion*" and "*mag*" denote where the values are taken, in the ionosphere or in the magnetosphere (Borovsky, 1993). W_{ion} is arc width

$$W_{ion} = W_{mag}\frac{B_{mag}}{B_{ion}}\frac{L_{mag}}{L_{ion}} \tag{10}$$

Most of arc auroral particles are precipitated from the same source region, B_{mag}/B_{ion} and L_{mag}/L_{ion} are not much different in different MLT, W_{ion} would be decreased as W_{mag} decreased. Magnetospheric source region of auroral arcs is maybe Boundary Plasma Sheet (BPS). This boundary layer is narrower as MLT is close to midday, so spatial scale of the auroral arc in magnetosphere W_{mag} would be smaller, and arc width W_{ion} would be smaller. But, distribution is more complex in the afternoon. In the afternoon, some elongated arcs are extending into the evening/nightside sectors (Meng and Lundin, 1986), and it has the activity feature of nightside aurora. So the postnoon auroral arcs are probably a mixture of dayside aurora and nightside aurora. The distribution curve of postnoon auroral arcs will be like that as shown in Fig. 6c, the number of wider arc (>10 km) is increased. These arcs might be the extensions of discrete auroras from nightside auroral oval.

Author's personal copy

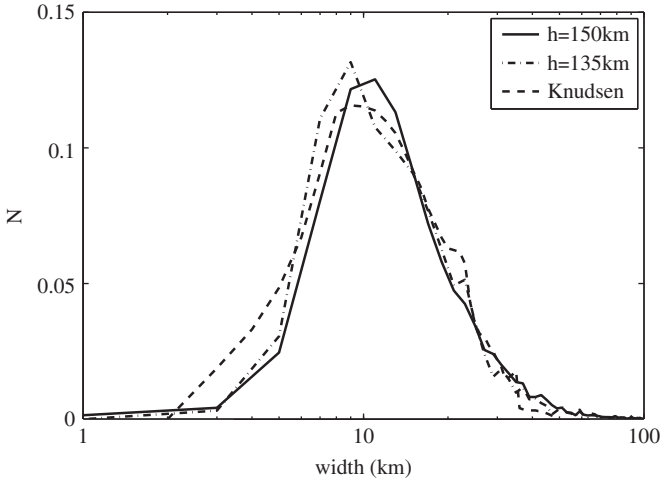

Fig. 7. Distributions of arc widths. The solid line and dashed-dotted line show respectively corrected widths at altitude of 150 km and those at altitude of 135 km. The dashed line shows the distribution from Knudsen et al. (2001).

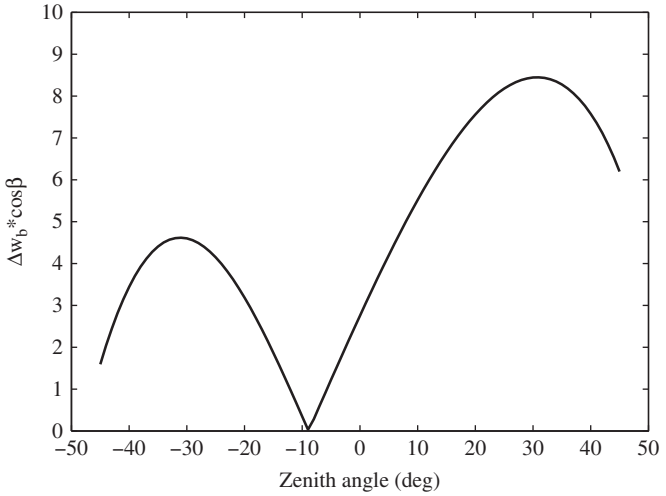

Fig. 8. The effect of bottomside emission scale height as a function of zenith angle.

5. Discussion

ASIs are taken with a 7 s exposure every 10 s. What is the influence of the exposure time on the measured FWHM? In Fig. 1b, the zenith angle of a peak is the position of the arc. The drift distance can be estimated by looking at the positions of an arc in one image and in another one taken 1 min later. Average drift distance in 1 min we calculated is 16 km giving an average moving speed of 0.27 km/s. The drift distance during exposure time is therefore about 1.9 km. It is less than the FWHM of most auroral arcs. This influence would not modify the distribution of widths.

In this paper, the auroral altitude is assumed to be 150 km. But auroral particles with different energies would precipitate at different altitudes. We measured FWHM at altitude of 135 km. Using least square fit, we obtained the altitudinal extent Δh as 28 km and k as 2.3 and 1.4 for the positive and negative geomagnetic zenith respectively. And then we could calculate the corrected width at altitude of 135 km. Comparing with the corrected width at altitude of 150 km, we find it is mostly (90%) 0.5–3 km smaller giving the average value of 1.7 km. Fig. 7 shows distributions of arc widths. The solid line and dashed-dotted line show respectively widths corrected by Eq. (8) at altitude of 150 km and those at altitude of 135 km. The dashed line shows the distribution from Knudsen et al. (2001). Comparing with dashed-dotted line ($h=135$ km), the shape of solid line ($h=150$ km) is the same, but the position of the peak is 2 km larger. This distribution is consistent with that of Knudsen et al. (2001) which corresponded to arcs that were observed near the geomagnetic zenith (for which observed widths are close to real widths). Thus, the hypothesis, which angle β varies linearly with zenith angle θ between -38° and 42°, could be accepted. Hence Eq. (8) could be used to obtain the real widths of the arcs from the observed ones. Some work about altitude extent of arcs had been done (Harang, 1946; Chamberlain, 1995). In Harang's study, the upper value of $l_{1/2}$ is the distance from luminosity maximum to the point where the luminosity had decreased to 1/2 of the maximum value on the upper part, and it is respectively 23.6 km and 30.8 km at altitude of 135 km and 150 km. Since the altitudinal extent Δh (30 km) is consistent with the upper value of $l_{1/2}$ (30.8 km) at altitude of 150 km, the height of auroral maximum luminosity we used in this paper is 150 km.

The altitude extent Δh in Eq. (3) is the topside emission scale height. We did not consider the effect of bottomside emission scale height Δh_b to correct arc width. But it would still affect arc width. It would add Δw_b to the observed width

$$\Delta w_b = \Delta h_b |\tan(\theta - \theta_{mz})| \tag{11}$$

Because intensity of auroral arc is the integral effect, we could just consider the effect of altitude extent closed to geomagnetic zenith. The factual added width is $\Delta w_b - w_1$. Combining Eqs. (5) and (6), bottomside emission scale height Δh_b would add dw ($=\Delta w_b \cos\beta$)–w_0 to w_0 (Fig. 8). If $dw > w_0$, dw would be thought to be the real width of arc w_0 by mistake. Here, Δh_b is assumed to be 18 km (Harang, 1946). In Fig. 8, it had two maximum values of dw: 4.6 km at -30° zenith angle and 8.4 km at 30° zenith angle. That is why average width near $\pm 30^\circ$ zenith angle is larger than that at other zenith angle in Fig. 4.

6. Conclusion

The conclusions of this study are as follows:

1. The observed width of the arcs increases regularly as zenith angle moves away from the geomagnetic zenith, because of the altitudinal extent of arcs and the effect of the angle β between the magnetic field and the LOS. A correction method is proposed to obtain real width of the arcs by considering these geometric effects.
2. The least square method was used to fit on the minimum and average FWHM curve to obtain two important parameters: the altitudinal extent Δh and the angle β.
3. The distribution curve of arc widths between -38° and 42° is consistent with that corresponded to arcs that observed near the geomagnetic zenith. The confidence interval is -38–42°. The width of the stable arcs taken within confidence interval is 18.5 ± 13 km.
4. The results suggest that the correction method for calculating arc width is valid.
5. The widths of dayside auroral arcs are narrower as MLT is close to midday. It is obvious in the prenoon sector. The postnoon auroral arcs are mixed dayside aurora with nightside aurora.

In summary, we propose a correction method to calculate the arc width, which can be extended to large zeniths, and more samples can be analyzed to study the relationship of width and intensity of arc. The evolution features of the arc width, distinction between different auroral arcs in the postnoon sector and probably

Author's personal copy

the acceleration mechanism in the magnetosphere, will be studied in a later paper.

Acknowledgments

This work was supported by the National Natural Science Foundation of China (41031064, 40974083, 41274164, and 41274149), the Foundation of Shaanxi Educational Committee (12JK0543), Ocean Public Welfare Scientific Research Project, State Oceanic Administration People's Republic of China (201005017), 973 Program (2010CB950503-06), and by the China Meteorological Administration Grant (GYHY201106011). Thanks for the funds supporting of Chinese Arctic and Antarctic Administration (10/11YR09).

References

Akasofu, S.-I., 1976. Recent progress in studies of DMSP photographs. Space Science Review 19, 169–215.

Borovsky, J.E., 1993. Auroral arc thicknesses as predicted by various theories. Journal of Geophysical Research 98 (A4), 6101–6138.

Borovsky, J.E., Suszcynsky, D.M., Buchwald, M.I., Dehaven, H.V., 1991. Measuring the thicknesses of auroral curtains. Arctic 44 (3), 231–238.

Chamberlain, J.W., 1995. Physics of the Aurora and Airglow. American Geophysical Union, Washington, D.C., pp. 128–132.

Harang, L., 1946. The auroral luminosity-curve. Terrestrial Magnetism and Atmospheric Electricity 51 (3), 381–400.

Hu, Z.J., Yang, H., Huang, D., Araki, T., Sato, N., Taguchi, M., Seran, E., Hu, H., Liu, R., Zhang, B., Han, D., Chen, Z., Zhang, Q., Liu, S., 2009. Synoptic distribution of dayside aurora: multiple-wavelength all-sky observation at Yellow River Station in Ny-Alesund, Svalbard. Journal of Atmospheric and Solar-Terrestrial Physics 71 (8–9), 794–804.

Kim, J.S., Volkman, R.A., 1963. Thickness of zenithal auroral arc over Fort Churchill, Canada. Journal of Geophysical Research 68 (10), 3187–3190.

Knudsen, D.J., Donovan, E.F., Cogger, L.L., Jackel, B., Shaw, W., 2001. Width and structure of mesoscale optical auroral arcs. Geophysical Research Letters 28 (4), 705–708.

Lui, A.T.Y., Anger, C.D., 1973. A uniform belt of diffuse auroral emission seen by the ISIS-2 scanning photometer. Planetary and Space Science 21, 799–809.

Maggs, J.E., Davis, T.N., 1968. Measurements of the thicknesses of auroral structures. Planetary and Space Science 16, 205–206.

Meng, C.-I., Lundin, R., 1986. Auroral morphology of the midday oval. Journal of Geophysical Research 91 (A2), 1572–1584.

Murphree, J.S., Cogger, L.L., Anger, C.D., Wallis, D.D., Shepherd, G., 1987. Oval intensifications associated with polar arcs. Geophysical Research Letters 14, 403–406.

Rostoker, G.A., Lui, A.T.Y., Anger, C.D., Murphree, J.S., 1987. North–south structures in the midnight sector auroras as viewed by the Viking imager. Geophysical Research Letters 14, 407–410.

Sandholt, P.E., Carlson, H.C., Egeland, A., 2002. Dayside and Polar Cap Aurora. Kluwer Academic Publishers, Dordrecht, pp. 14–15.

Stenbaek-Nielsen, H.C., Hallinan, T.J., Peticolas, L., 1999. Why do auroras look the way they do? Transaction American Geophysical Union (EOS) 80, 193–199.

Yang, H., Sato, N., Makita, K., Kikuchi, M., Kadokura, A., Ayukawa, M., Hu, H.Q., Liu, R.Y., Häggström, I., 2000. Synoptic observations of auroras along the postnoon oval: a survey with all-sky TV observations at Zhongshan, Antarctica. Journal of Atmospheric and Solar-Terrestrial Physics 62, 787–797.